NPA/Int. 69-2
22.1.69

MEASUREMENT OF GROWTH RATE FOR SUB-VISIBLE BUBBLES IN A BUBBLE CHAMBER

by

G. Harigel, H.J. Hilke, A. Rogers, CERN, Geneva
G. Horlitz, S. Wolff, DESY, Hamburg
E. Fretwurst, G. Lindström, I. Institut für Experimentalphysik der Universität Hamburg

1. Introduction

An increasing interest in fast cycling bubble chambers has made evident the need for experimental data concerning bubble growth and collapse rates. Theoretically, it is known that in the limit of large bubble radii well above the critical radius and below about one mm the process is heat limited and varies like $r \sim t^{1/2}$. A recent experiment conducted with the hydrogen bubble chamber at DESY [1] has checked this dependence and found good agreement for radii down to 40 microns, corresponding to times of roughly 100 microseconds (for a large chamber, this is the limit of measurability and almost the limit of visibility). For certain applications (e.g. ultrasonically driven bubble chambers) one needs to know the bubble growth characteristics at much shorter times, on the order of 20 microseconds or less. In order to measure the growth rate of sub-visible bubbles, one of the authors (A.R.) proposed to use the resonance absorption of high frequency sound.

---

1) G. Harigel, G. Horlitz, S. Wolff, DESY 67/14

2) G.T. Trammel, J. Appl. Phys. Vol. 33, No 5, May 1962, p. 1662. (Note that we differ only by a factor of 1/3, which we assume is misprinted in his article).

2. Theory

The following is a synopsis of the theoretical considerations related to resonant absorption of sound by vapour bubbles [2].

We begin by considering a sound wave of sufficiently high frequency that the bubble properties vary only slightly in one period. Under these conditions and defining the bubble compressibility K_b by

$$\frac{\Delta V}{V} = K_b \, \Delta p,$$

one obtains

$$K_b = \frac{1}{\rho_v C_v^2} + \frac{3\lambda}{\rho_v L_v \frac{dp_v}{dT}} \left[\frac{1}{R} \left(\frac{\pi}{\alpha\omega}\right)^{1/2} . e^{\frac{i\pi}{4}} + \frac{i}{R^2} \right] \qquad (1)$$

(ρ_v, C_v, L_v, and p_v are density, sound velocity, latent heat of vaporization and equilibrium pressure of the vapour : ρ_L, λ and C_p the density, thermal conductivity and the specific heat of the liquid; T is the temperature, ω the frequency and R the bubble radius).
For simplicity we express this as

$$K_b = \left[1 + \frac{A}{\omega^{1/2}.R} \left(1 + i + \frac{Bi}{\omega^{\frac{1}{2}}.R}\right) \right] .C \qquad (2)$$

where A, B and C are merely combinations of the constants. Next, one must determine how the bubble compressibility alters the effective compressibility (and hence propagation of sound) in the liquid. Defining the pressure as the sum of a plane wave and a radial wave centered on an individual bubble,

$$p = p_o \, e^{ikr} + p_{so} \cdot \frac{e^{ikr}}{r}$$

we find

$$p_{so} = \frac{\rho_L R^3 \omega^2 \cdot \frac{K_b}{3} \cdot p_o}{1 - \rho_L \omega^2 \frac{K_b R^2}{3} (1-ikR)^{-1}} \qquad (3)$$

From this one can show that as long as the total volume of bubbles is a small fraction of the liquid volume, the altered propagation constant will be

$$(k')^2 = k^2 + 4\pi n \frac{p_{so}}{p_o} = k^2 + \frac{4\pi n \omega^2 R (1-ikR)}{\omega^2 - \frac{3(1-ikR)}{R^2 K_b \rho_L}} \qquad (4)$$

In situations where kR may be neglected compared to one as for bubble radii and frequencies that we are interested in, this reduces to

$$\delta k = -2\pi n C_L \frac{\omega R}{\omega^2 - \frac{\frac{3}{C}(1+\frac{A}{\omega^{\frac{1}{2}}R})}{R^2\rho_L (1+\frac{A}{\omega^{\frac{1}{2}}R})^2 + (\frac{A}{\omega^{\frac{1}{2}}} + \frac{A.B}{\omega R^2})^2} + \frac{\frac{3i}{C}(\frac{A}{\omega^{\frac{1}{2}}R} + \frac{A.B}{\omega R^2})}{R^2\rho_L (1+\frac{A}{\omega^{\frac{1}{2}}R})^2 + (\frac{A}{\omega^{\frac{1}{2}}R} + \frac{A.B}{\omega^{\frac{1}{2}}R\,\omega R^2})^2}} \qquad (5)$$

where C_L is the velocity of sound in the liquid and n is the number of bubbles per unit volume, The real part of δk gives the change of sound velocity due to the presence of the bubbles, the imaginary determines the absorption. Maximum absorption one gets when the real part of the denominator is zero.

3. Design

Three crystals (piezoelectric transducers PZT5A from Brush Clevite) of dimensions 50 mm x 12 mm x 3 mm were parallel mounted 2 mm apart, as shown in figures 1 (a) and 2. The resonance frequency was f = 122 Kc/sec. Downstream from the beam a pair of small counters defined the slit between crystal 1 and X; that is, it produced a trigger pulse whenever a track passed through this slit. The beam intensity was sufficiently weak that there was negligible chance of a track passing simultaneously through slits 1 - X and 2 - X. Our technique consisted in driving crystal X with a wave train beginning just prior to the arrival of the beam and receiving on crystal 1 and 2. The output from 1 and 2 was externally balanced so that initially their difference signal was quite small. Whenever a track passed through the 1 - X slit, the bubbles produced served to attenuate the signal reaching crystal 1, and this gave a difference signal which

varied in amplitude according to the average bubble radius. The sum of this difference signal and the initial (static) difference was then amplified and displayed on an oscilloscope. It was necessary to strongly suppress lower sound frequencies being produced by the expansion system.

The oscilloscope was triggered by a coincidence signal from the two Lithium-drifted Silicon detectors C_1 and C_2. Considerable difficulty arose from the fact, that these detectors had to be mounted sufficiently close to the crystal arrangement 1,X,2 in order to define the electron beam cross section with good accuracy. A special vacuum tube was used which served as housing for the detectors inside the bubble chamber. The distance between the detectors was chosen to be 55 mm, while the distance from the closest detector to the centre of the crystal arrangement 1,X,2 was 68 mm.

The detectors were cut in dimensions 3 x 3 mm from a larger slab in which a compensated intrinsic zone of 3.5 mm depth was produced by conventional Lithium-drift technique.

Due to the experimental arrangement the detectors were cooled down to about hydrogen temperature during the experiments and therefore the thermal noise of the detectors was negligible. Instead, the total system noise was entirely determined by the preamplifier input capacity of 520 pF due to the cable length between detector and preamplifier which gave a noise of 30 keV rms. After amplification and shaping fast discriminators were used to set a discrimination level as low as possible below the maximum of the Landau distribution.

In a preliminary test a silicon surface barrier detector with a thickness of about 500 μ was exposed to a 5 GeV electron beam outside the bubble chamber. The obtained spectrum which was also representative for all further experiments is shown in Fig. 3 and exhibits a typical Landau-distribution.

4. Operating Conditions

A test could be arranged in the piston-expanded 85 cm bubble chamber at DESY at a time, when the chamber was used to test Ne - H_2 mixtures. This caused some more difficulties for the evaluation because some thermodynamical properties of the mixture are not accurately known. The chamber conditions were as follows: 92 mole % Neon and 8 mole % H_2, liquid temperature = 29.0° K, expanded (final) pressure = 2.0 atmospheres. We used crystals with a frequency of 122 Kc/s. The driving voltage on crystal X was 5 Volts, hence the sound amplitude and the heating by the crystal should have contributed negligibly to the bubble growth. One difficulty which we had foreseen was the possibility of spurious bubbles originating between the crystals, or else starting on the crystal edges or the mount and being carried by the liquid into either slit 1 - X or 2 - X. This could result in a spurious, time dependent difference signal. Every effort was made to polish any rough surfaces connected with the crystals or mounts, and the photographs taken during operation of the chamber indicate that these precautions were sufficient. No spurious bubbles were seen to originate in either slit, and those originating outside took a very long time (in terms of the rates we are considering) to drift between the crystals. Moreover, by triggering the oscilloscope on occasions when no track was detected in the 1 - X slit, we found a a difference signal (from the slight imbalance between 1 and 2) which was constant in time.

5. Results

We have analysed in detail the three oscilloscope photographs which appear in Figure 4. Depending on the sign of the initial difference signal the signal related to bubble growth may either add (4 a) or subtract (4 b, 4 c). The reduced data from these three pictures is presented on the graph in Figure 5, where we have plotted the difference voltage (relative to its maximum value) versus time. From equation (5) it is possible to calculate values of the difference signal as a function of bubble radius. For this calculation the

phase change due to the change in the sound velocity as well as the absorption, that is the real and the imaginary part of δ , have to be taken into account. Now, by assuming the dependence $r \sim t^{1/2}$, and joining the curves at the point of maximum attenuation (22 microseconds from oscilloscope pictures, 28.5 microns resonance-radius for the theory), one gets reasonably good agreement. For times less than about 15 microseconds the data suggests a bubble radius somewhat larger than that predicted by the $t^{1/2}$ curve, which is to be expected since the initial stage of growth is much faster and not dependent on heat transfer. However, the accuracy of the data - especially in this region - is not sufficient to warrant more quantitative conclusions.

As a check on this analysis, one can simply predict that the bubble radius will be 192 microns at 1 millisecond assuming $r \sim t^{1/2}$; measurements of the bubbles from photographs give the same order of magnitude.

6. Conclusions

The technique works quite acceptably, and as the apparatus is neither expensive nor complicated it suggests several areas of application. Principally it is useful for measuring the effect of changing the operating conditions in a chamber on the initial growth and final collapse of bubbles. Such measurements are crucial for rapid cycling, since the time it takes for a bubble to totally disappear, leaving no nucleation centres for subsequent expansions, ultimately is the limit on any cycling rate. The choice of frequency for the crystals used in this method determines the range of bubble radii which give maximum attenuation; hence higher frequencies will better resolve smaller bubbles.

Finally, the error on the data points is due mainly to sounds in the chamber being produced by the expansion system and picked up by the crystals, and can be reduced below what we have obtained on this trial.

Acknowledgements

We are greatly indebted to Dr. C.A. Ramm and Professors W. Jentschke and M.W. Teucher for their interest in the investigations and financial help. We also thank H. Ancey for the construction of the crystal assembly and the bubble chamber team for the valuable help during preparation and running of the experiment, especially W. Eschricht, H.J. Fiebig, U. Knopf, G. Kunst, D. Nowakowsky, O. Peters, and W. Stahlschmidt. One of us (H.J.H.) has to thank the Ministerium für wissenschaftliche Forschung, Bonn, for financial support.

Distribution : (open)
Scientific Staff of NPA Division

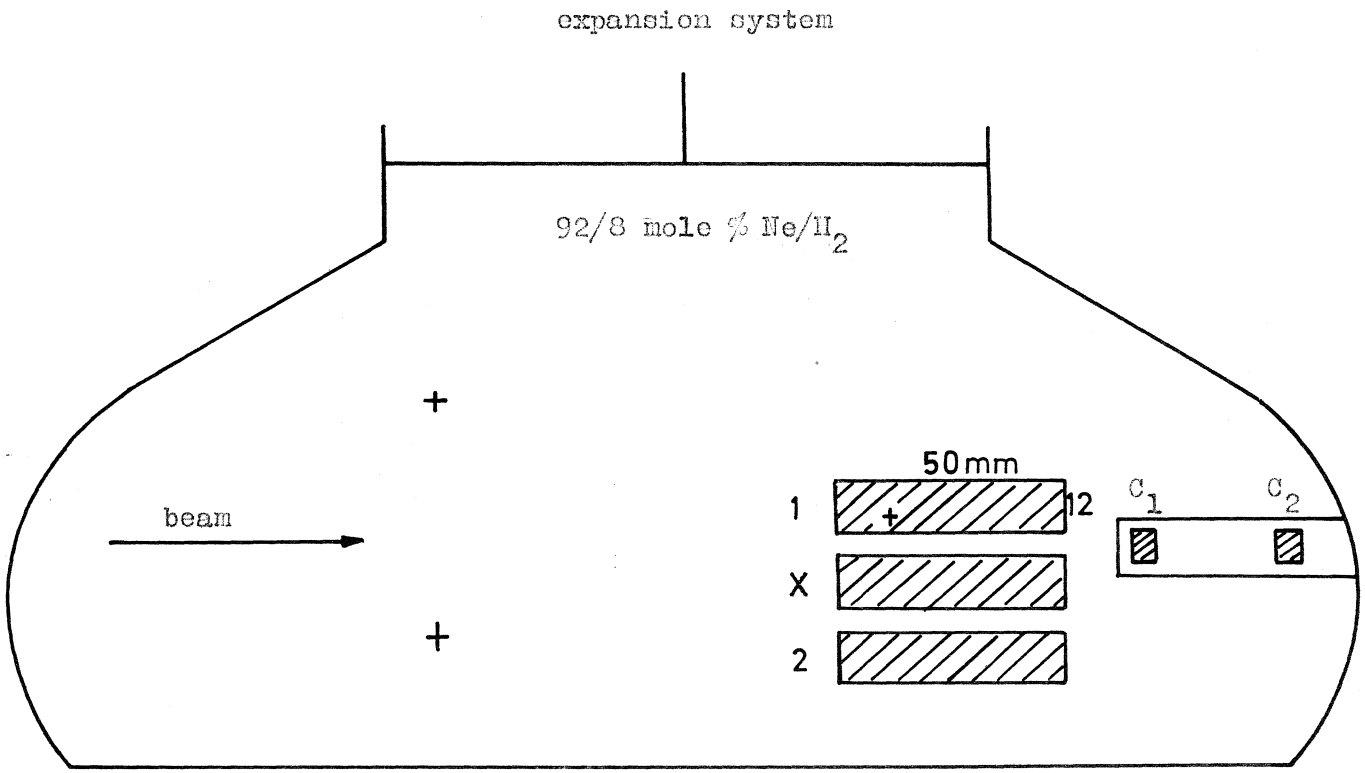

Fig. 1

schematic: bubble chamber with ultrasound crystals

1,X,2; counters C_1, C_2 and camera axes (+)

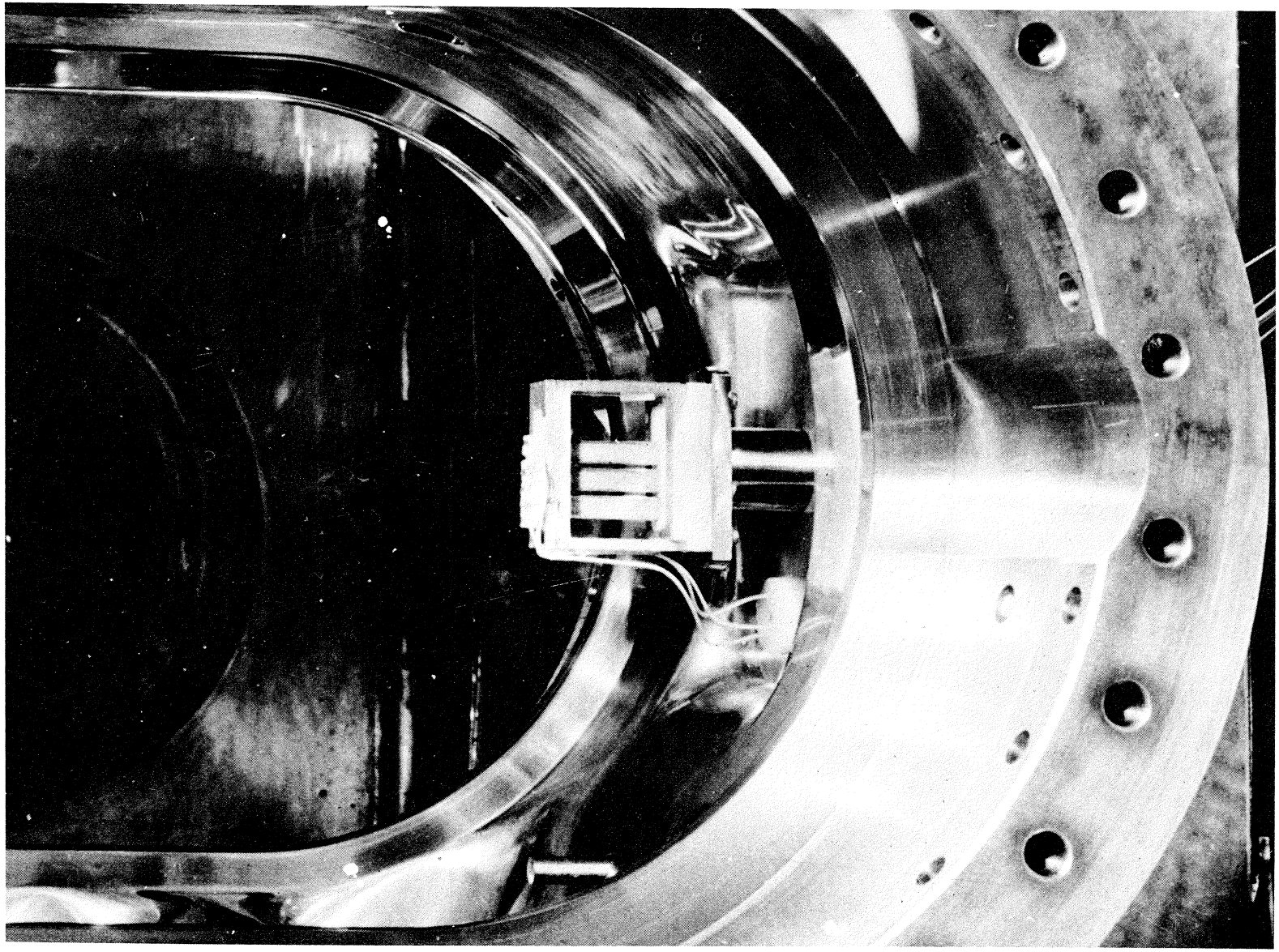

Fig. 2 Photo showing the crystal assembly mounted in the bubble chamber

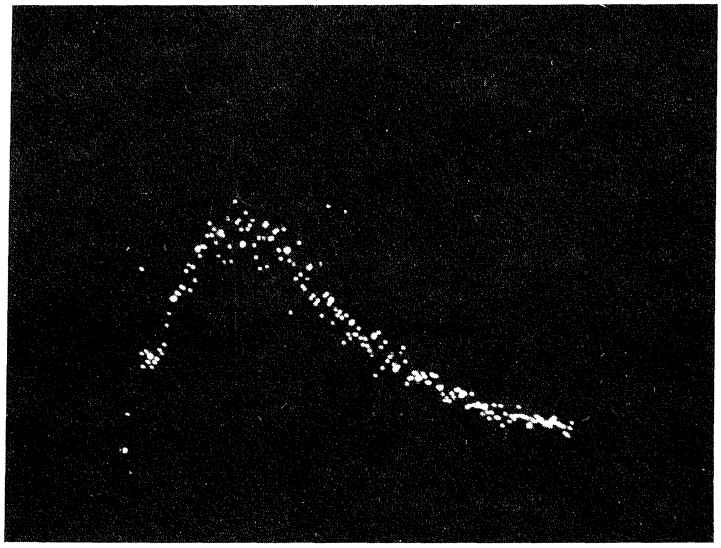

Fig. 3

Pulse-spectrum from the Silicon
detectors with 5 GeV electrons

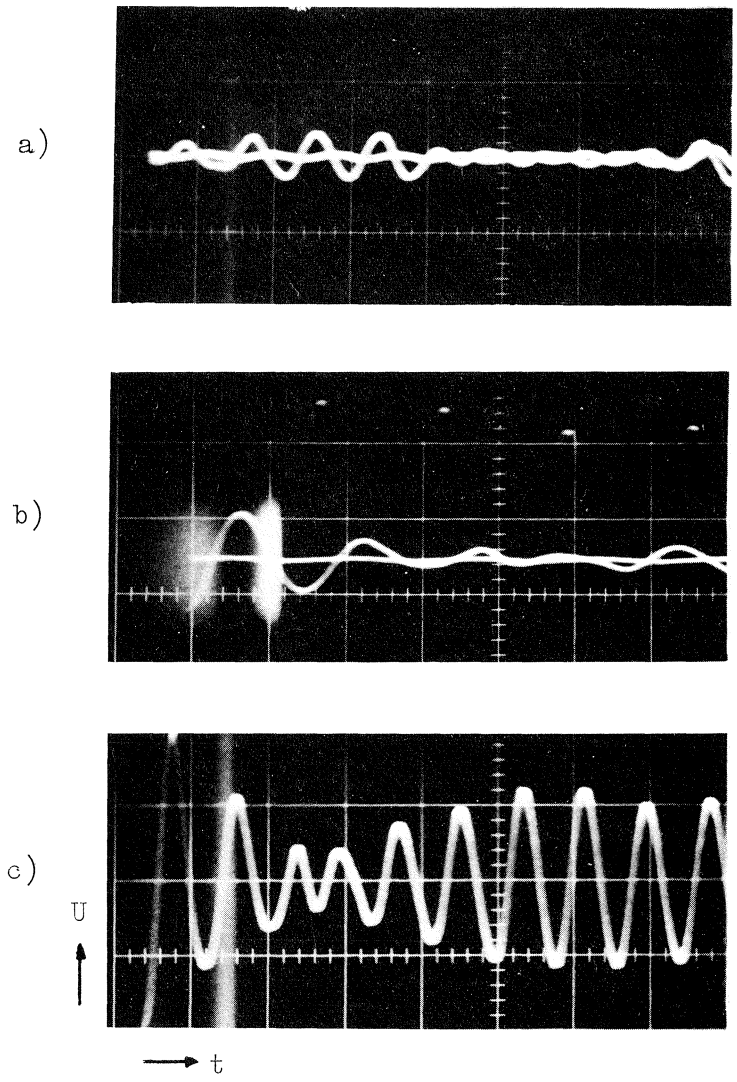

Fig. 4

Amplified difference-signal from crystals 1 and 2, t = 10 µs/cm (a,c) and 5 µs/cm (b); U = 0.2 V/cm

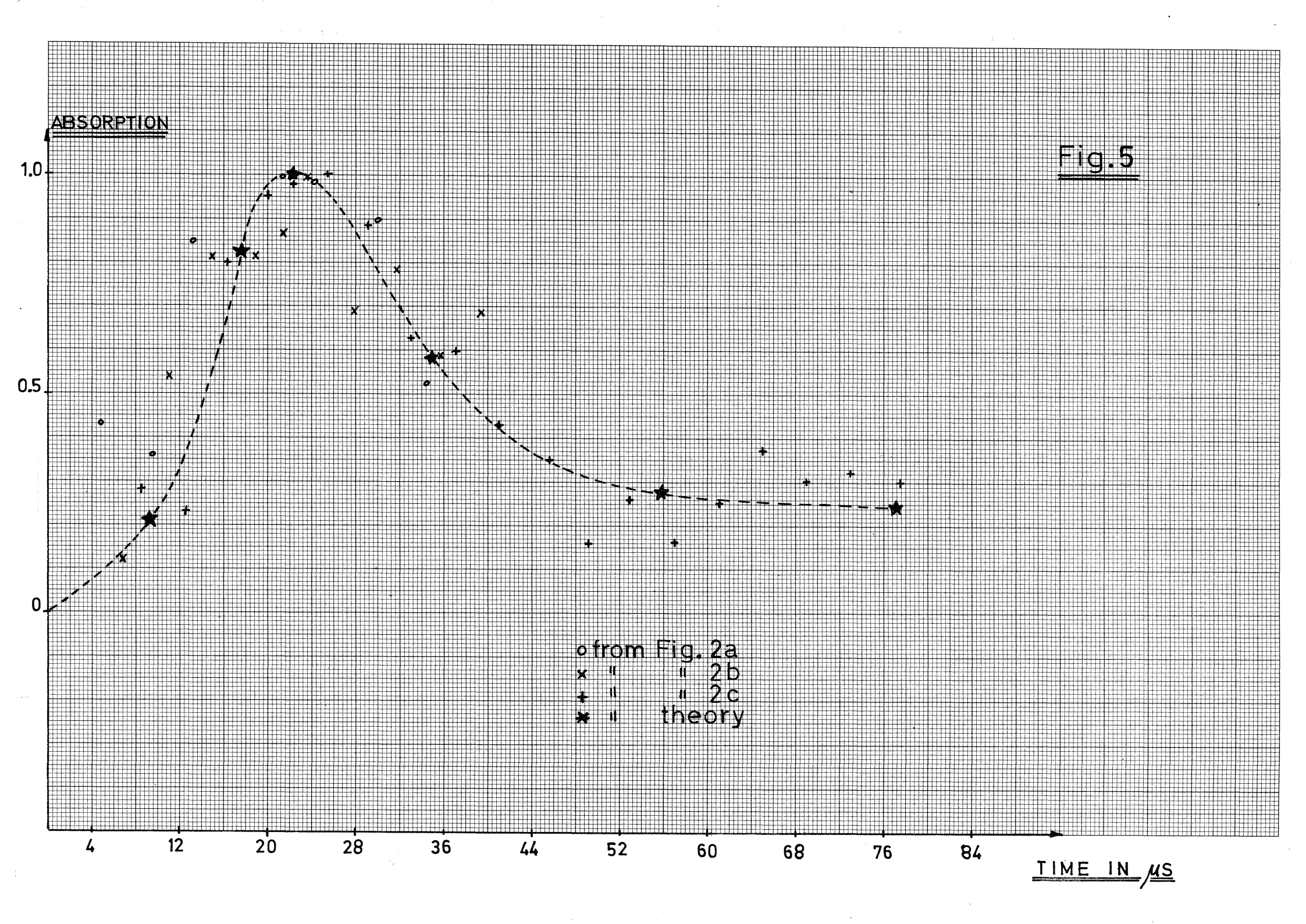
ABSORPTION
1.0
0.5
0
4
12
20
28
36
44
52
60
68
76
84
TIME IN μS
o from Fig. 2a
× " " 2b
+ " " 2c
✱ " theory

Fig. 5